SYRINGE-ASSISTED POINT-OF-CARE PUMPING

L. Xu, H. Lee, and K. W. Oh

SMALL (Sensors and MicroActuators Learning Lab), Department of Electrical Engineering,
University at Buffalo, The State University of New York (SUNY at Buffalo),
Buffalo, New York 14260, USA, kwangoh@buffalo.edu

1. ABSTRACT

This paper presents a convient pumping method by only employing a hand held syringe. Due to the gas permeability of polydimethylsiloxane (PDMS), air trapped in the flow channel can be diffused into the surrounding vacuumed chammbers through the PDMS gaps between them. Thus after loading sample liquids, a constant flow was realized, whose flow rate can be controlled by the gap distance and overlap area between a dead-end channel and a surrounded chamber of the PDMS devices. Moreover, in order to realize a point-of-care application, the surrounded chamber was vacuumed by a hand-held syring. Therefore by pulling a syring only by hand, a constant flow rate ranging from 0.3 nl s^{-1} to 4 nl s^{-1} was realized in our experiment.

Keywords: Point-of-care, polydimethylsiloxane (PDMS), micropump

2. INTRODUCTION

How to realize point-of-care pumping is always the key issue to be solved in point-of-care diagnostics. Currently, most of the point-of-care pumping methods are employing passive ways based upon capillary force [1]. Due to capillary force is mainly relied on the property of the surface and the testing liquids, flow rate is generally hard to control[2].

Another widely used method is employing electrokinetic [3]. Powered by external electrical sources, various flow rates can be realized by adjust the electric field. While also due to the induced high electric field, these methods are not suitable for a lot of bio-samples. Moreover this kind of method is usually only suitable for glass-based microfluidic devices.

Thus an alternative method by utilizing the high gas permeability of PDMS has been considered as a promising way. High gas permeability of PDMS is one of unique properties of PDMS [4]. This has allowed easy removal of trapped air bubbles out of microchannels[5, 6]. In addition, vacuum-assisted self-powered pumping has been introduced by [7]: Firstly, PDMS devices were place in a vacuum chamber to pre vacuumed the whole devices. Secondly, after the PDMS devices are degassed at low pressure, they will re-absorb air to reach a new equilibrium if they expose to atmosphere. Thus by loading liquid at the inlet port of a dead-end channel, the fluid can be drawn into the channel. Moreover, by adding two different types of liquids, microchip immunoassay was realized [8]. Based on the same principle, this method has been utilized for a self-powered microfluidic blood analysis system [9, 10] and a viscometer [11].

Although the vacuum-assisted degas-driven flow is convenient to use without external pumps, there are still several practical limitations: (1) Before a device can work as a pump, it needs to be stored in a vacuum chamber for more than one hour to degas the PDMS bulk; (2) After the device is exposed to air, its pumping ability decays exponentially with time, so that it should be used right after the pre-evacuation; (3) In general, the flow rate generated from the vacuum-assisted flow is nonlinear and uncontrollable; (4) In order to increase the flow rate and keep it constant, a large dead volume is needed at the end of the channel. This in turn, needs more sample liquid to fill the entire channel.

Thus instead of pre-evacuate the whole device, a low pressure source was connected to the end of the channel while separated by a thin PDMS membrane by adopting a sandwich-like structure: flow channel on top layer, low pressure source at bottom layer and between them is the membrane [12]. By controlling the thickness and area of the membrane, different flow rates were realized. While the process to make this kind of sandwich structures is not easy usually requires the alignment between the top and bottom layers. Plus it is relatively hard to control the PDMS membrane thickness and uniformity. To overcome these limitations of using the vacuum-assisted pumping, we have designed a simple syringe-assisted pumping method. In this paper, we have systematically investigated the major parameters (e.g., gap distance, overlap area) that can generate constant and controllable flow rates.

3. THEORY

As shown in **Figure 1**, a dead-end channel is partly surrounded by a chamber with a thin gap distance. Firstly, a glass syringe is connected with the chamber by a tube. By pulling the plunger, low pressure will be generated inside the chamber, where cylindrical posts are placed to prevent the collapse of the chamber at low pressure. Liquid is loaded in the inlet port after waiting a few seconds to allow constant and steady-state air flux. The pressure difference between the dead-end channel and the surrounded chamber allows air diffusion through the gas-permeable PDMS, from inside the channel to the chamber across the gap. Therefore, the fluid can be drawn inside the dead-end channel. This

approach facilitates a straightforward point-of-care pumping system that does not require pre-evacuation of PDMS devices in a vacuum chamber.

A rough estimate of the characteristic time to allow for the constant and steady-state air flux across the thin gap distance (g) can be obtained by examining the diffusion time (t_D) across the PDMS gap distance: $t_D \approx g^2 D^{-1}$, where D is the diffusion coefficient of air in PDMS. For example, if g = 50 μm and $D = 3.4\times10^{-9}$ m^2 s^{-1}, the characteristic time to initialize the steady-state air flux is $t_{D1} \approx 0.74$ sec. Another characteristic time to diminish the steady-state air flux would depend on the air diffusion from the surface into the chamber across the thick PDMS layer (e.g., ~ 5 mm), which is $t_{D2} \approx 2$ hours. Therefore, the air flux will be kept steady and constant if devices are operated within $t_{D1} << t << t_{D2}$.

According to Fick's diffusion law,[7, 11] we can get an approximate value of the steady-state flux F (mol m^{-2} s^{-1}) of air that diffuses into the chamber across the gap distance through the gas-permeable PDMS

$$F = -D\frac{\Delta C(x)}{\Delta x}\bigg|_{x=g} \approx D\frac{C(0)-C(g)}{g} = D\frac{C_{\text{PDMS}}-C_{\text{Chamber}}}{g} \quad (1)$$

where $C(x)$ is the air concentration profile in PDMS across the gap distance (**Figure 1c**). The initial air concentration inside the dead-end channel and chamber is C_{ATM} = 44 mol m^{-3}.[4, 11] The air concentration saturated in bulk PDMS is known to be C_{PDMS} = 4.89 mol m^{-3} at atmosphere. The large volume expansion in the syringe (e.g., 1.6 μl to several hundred μl) will initiate a new equilibrium air concentration inside the chamber: C_{Chambe} = 0.35 mol m^{-3} for the volume expansion to 200 μl. After t_{D1}, the air concentration at $x = g$ will be depleted to $C(g) = C_{\text{Chamber}}$, while the air concentration at x = 0 will be $C(0) = C_{\text{PDMS}}$ (**Figure 1d**). Thereafter, the air flux F will be kept constant if operated within $t_{D1} << t << t_{D2}$: the waiting time of 5 sec ($t >> t_{D1}$) and the whole pumping time of less than 8 min ($t << t_{D2}$).

The syringe-assisted air flux causes the degas-driven flow in the dead-end channel. If we assume that the air concentration or the air density inside the channel is unchanged during the pumping process, the volumetric flow rate (Q) and the pumped fluid volume (V) inside the channel can be expressed as

$$Q(t) \approx k\frac{F\,S(t)}{C_{\text{ATM}}} = k\,D\frac{C_{\text{PDMS}}-C_{\text{Chamber}}}{C_{\text{ATM}}}\frac{S(t)}{g}$$
$$\Rightarrow V(t) = \int Q(t)dt \quad (2)$$

where k is an empirical factor related to viscous effect of the pumped liquid flow and $S(t)$ is the total surface area that allows air to diffuse into the PDMS bulk that equals the overlap area of the channel and chamber. **Equation 2** points out that there are two major parameters that can affect the flow rate: the gap distance (g) and the overlap surface area (S_0) between the channel and chamber.

4. DESIGN AND FABRICATION

4.1 Design

In order to study the relationships between the flow rate Q and these two parameters, two sets of devices are designed (**Figure 2a** and **Figure 3a**). In the first set, five different devices are designed with different gap distances (e.g., 25, 50, 100, 200 and 300 μm), while the overlap area is kept the same (S_0 = 0.28 mm^2). In the second set, five different devices are made with different overlap areas (e.g., 0.00345, 0.176, 0.521, 0.693 and 0.866 mm^2), while the gap distance is kept unchanged (g = 50 μm). In both two sets, channels and chambers have the same height (h = 34.5 μm) and all the channels have the same width (w = 100 μm).

4.2 Microfluidic device fabrication

All devices were fabricated by a standard soft lithography process. [13]. A 3 inch silicon wafer with one side polished (University wafers, South Boston, MA, USA) was submerged into BHF (buffered hydrofluoric acid) at room temperature for 5 min to remove the thin native silicon dioxide layer. After that, the wafer was cleaned by using acetone, methanol respectively and then rinsed in deionized water before blown dry by filtered nitrogen gas. After cleaning, the cleaned wafer was placed on a hot plate at 120°C for 5 min in order to make it completely dehydrated. SU-8 (SU-8 2050, Micro-Chem Corp, Newton, MA, USA) was then spin coated on top of the wafer by using the spin coater (WS-650Mz NPP from Laurell Technologies, North Wales, PA, USA) to the target thickness. After spin coating, soft bake was performed on a leveled hot plate for 3 min and 9 min at 65°C and 95°C, respectively. After soft bake, UV photolithography was carried out by using a contact mask aligner. After UV exposure, the post exposure bake (PEB) was conducted on the leveled hot plate for 2 min and 7 min at 65°C and 95°C, respectively, followed by development in SU-8 developer for 5 min. After developing, the wafer was cleaned with isopropyl alcohol. Finally, the wafer was blown dry with filtered nitrogen gas and then placed on the hot plate at 100°C for 5 min to evaporate any residual of isopropyl alcohol.

A monomer of PDMS (Sylgard 184, Dow Corning) and corresponding curing agent was thoroughly mixed at a ratio of 10 : 1 (wt/wt). Then the mixed PDMS was degassed in a vacuum chamber for 20 min to remove all the air-bubbles. In order to peel off the PDMS from the wafer mold easily, hexamethyldisilazane (Sigma Aldrich, Saint Louis, MO, USA) was silanized on the surface of the wafer mold in vacuum chamber at room temperature for 30 min. After that the PDMS mixture was carefully poured onto the wafer

mold and then cured at 80°C for 3 hours. After PDMS was cured and peeled off from the wafer mold, holes were punched on the PDMS replicas for the connection with the syringe, followed by oxygen plasma treatment for irreversible bonding between PDMS and glass slide. Lastly, the device was baked over a hot plate for 48 hours at 70 °C to improve the bonding strength and stabilize the surface property of the devices.

5. TEST SETUP AND PROCEDURE

The fabricated microfluidic device was connected through a silicone tube to a glass syringe with maximum volume of 200 µl. The glass syringe was used to generate the low pressure inside the chamber of the fabricated microfluidic devices. All of the devices were tested three times. First, the syringe was pulled to have volume expansion to 200 µl. After pulling the plunger, DI water was loaded at the inlets after around 5 seconds. All the flow processes were recorded by a Nikon stereo-type microscope and camera set. By analysing the recorded video clips, volume-time curves were plotted. (KDS100W, Fisher Scientific, IL, USA).

6. RESULTS AND DISCUSSION

As shown in **Figure 2b**, before liquid reaches the part of the channel surrounded by the chamber, the liquid volume V is linear to the pumping time t, which indicates that the flow rate Q remains constant (Phase I). As the flow enters the part of the channel surrounded by the chamber after a certain time t_C, however, the flow rate exponentially decreases (Phase II).

When $t < t_C$ (Phase I), the overlap area will be a constant value: $S(t) = S_0 = 0.28$ mm^2. Thus, according to **Equation 2**, the flow rate Q_I and V_I can be written as

$$Q_{\mathrm{I}}(t) \approx k\frac{F\,S_0}{C_{\mathrm{ATM}}} = k\,D\frac{C_{\mathrm{PDMS}} - C_{\mathrm{Chamber}}}{C_{\mathrm{ATM}}}\frac{S_0}{g}$$

$$\Rightarrow V_{\mathrm{I}}(t) = Q_{\mathrm{I}}\,t = k\frac{F\,S_0}{C_{\mathrm{ATM}}}t$$

(Phase I: $t < t_C$) (3)

Therefore, as shown in **Figure 2c**, the flow rate Q_I in Phase I was constant at the given gap distance and proportional to g^{-1}. The empirical factor was $k = 0.57\pm0.03$, which indicates pumping power loss of 43% due to the viscous effect.

On the other hand, when $t > t_C$ (Phase II), the overlap area will be reduced and become time-dependent because the pulled-in liquid will block the part of the surface where the air can diffuse: $S(t) = S_0 - \Delta S(t)$, where $\Delta S(t) = 2\times h\times y(t) = 2\times w^{-1}\int Q_{\mathrm{II}}(t)\,dt$, and h and w are the height and the width of the channel, respectively. Thus, by solving a differential equation according to **Equation 2**, the flow rate Q_{II} and V_{II} can be written as

$$Q_{\mathrm{II}}(t) \approx k\frac{F\,S_0}{C_{\mathrm{ATM}}}e^{-\frac{t-t_C}{\tau}}$$

$$\Rightarrow V_{\mathrm{II}}(t) = k\frac{F\,S_0}{C_{\mathrm{ATM}}}t_C + \frac{w S_0}{2}\left(1-e^{-\frac{t-t_C}{\tau}}\right)$$

(Phase II: $t > t_C$) (4)

where τ is the time constant, $\tau = (w\times C_{\mathrm{ATM}})/(2\times k\times F)$. **Equation 4** explains the exponential decay of the volumetric flow rate $Q_{II}(t)$ and the pumped total volume $V_{II}(t)$ in Phase II, as shown in **Figure 2b**. The time constant τ is proportional to the gap distance (g).

Similarly, we investigated the syringe-assisted pumping related to the overlap area, while the gap distance was kept unchanged (g = 50 µm), as shown in **Figure 3a**. The pumped total volume was plotted in **Figure 3b**. In Phase II, exponential decay was shown with the same time constant τ for different overlap areas. This is due to the fixed gap distance, resulting in the same air flux F for all cases. The flow rate of the device with zero overlap distance ($S_0 = w\times h = 0.0035$ mm^2) was extremely low (0.089 nl s^{-1}), taking ~9 min to draw-in water completely. As only the very end of the channel was overlap with the chamber, the pumped total volume was linear with time during the whole pumping process (**Figure 3c**). In Phase I, as expected from **Equation 3**, the flow rate Q_I was linearly proportional to the overlap surface area (**Figure 3d**).

When $t \approx t_{D2}$, the syringe-assisted pumping will stop because the pressure difference completely vanishes inside the chamber due to the air diffusion from outside to the chamber. However, we can restore the low pressure or vacuum inside the chamber by simply reconnecting the syringe and pulling the plunger again. Therefore, unlike the vacuum-assisted degas-driven flow, the proposed syringe-assisted method permits instantaneous, recurring, point-of-care pumping. Another advantage of the syringe-assisted pumping is that the air diffusion is bi-directional between the channel and chamber depending on the polarity of pressure difference. By pushing the plunger, the drawn-in liquid solution can be retrieved from the dead-end channel. Thus, the syringe can supply not only *a vacuum source* (e.g., low pressure) but also *a pressure source* (e.g., high pressure) to drive the fluid flow *into* and *from* the dead-end channel. This will enable a simple point-of-care pumping system that requires multiple incubations and washing processes, which is under investigation and will be reported later.

7. CONCLUSION

By adjusting the gap distance and overlap area between the channel and chamber, we have controlled the flow rate and generated a constant flow before the fluid reaches the part of channel surrounded by the chamber. By the proposed method, a syringe-assisted, instantaneous, recurring, bi-directional, point-of-care pumping system

without external pumps or vacuum chambers has been realized with controllable flow rate ranging from 0.3 nl s^{-1} to 4 nl s^{-1}.

ACKNOWLEDGEMENTS

This work was partially supported by grants from NSF (ECCS-1002255 and ECCS-0736501).

REFERENCES

[1] L. Gervais and E. Delamarche, "Toward one-step point-of-care immunodiagnostics using capillary-driven microfluidics and PDMS substrates," *Lab on a Chip*, vol. 9, pp. 3330-3337, 2009.

[2] J. Ziegler, M. Zimmermann, P. Hunziker, and E. Delamarche, "High-Performance Immunoassays Based on Through-Stencil Patterned Antibodies and Capillary Systems," *Analytical Chemistry*, vol. 80, pp. 1763-1769, 2008/03/01 2008.

[3] J. M. Karlinsey, "Sample introduction techniques for microchip electrophoresis: A review," *Analytica Chimica Acta*, vol. 725, pp. 1-13, 2012.

[4] T. C. Merkel, V. I. Bondar, K. Nagai, B. D. Freeman, and I. Pinnau, "Gas sorption, diffusion, and permeation in poly(dimethylsiloxane)," *Journal of Polymer Science Part B: Polymer Physics*, vol. 38, pp. 415-434, 2000.

[5] W.-L. Ong, K.-C. Tang, A. Agarwal, R. Nagarajan, L.-W. Luo, and L. Yobas, "Microfluidic integration of substantially round glass capillaries for lateral patch clamping on chip," *Lab on a Chip*, vol. 7, pp. 1357-1366, 2007.

[6] J. H. Sung, C. Kam, and M. L. Shuler, "A microfluidic device for a pharmacokinetic-pharmacodynamic (PK-PD) model on a chip," *Lab on a Chip*, vol. 10, pp. 446-455, 2010.

[7] K. Hosokawa, K. Sato, N. Ichikawa, and M. Maeda, "Power-free poly(dimethylsiloxane) microfluidic devices for gold nanoparticle-based DNA analysis," *Lab on a Chip*, vol. 4, pp. 181-185, 2004.

[8] K. Hosokawa, M. Omata, K. Sato, and M. Maeda, "Power-free sequential injection for microchip immunoassay toward point-of-care testing," *Lab on a Chip*, vol. 6, pp. 236-241, 2006.

[9] I. K. Dimov, L. Basabe-Desmonts, J. L. Garcia-Cordero, B. M. Ross, A. J. Ricco, and L. P. Lee, "Stand-alone self-powered integrated microfluidic blood analysis system (SIMBAS)," *Lab on a Chip*, vol. 11, pp. 845-850, 2011.

[10] D. Y. Liang, A. M. Tentori, I. K. Dimov, and L. P. Lee, "Systematic characterization of degas-driven flow for poly(dimethylsiloxane) microfluidic devices," *Biomicrofluidics*, vol. 5, pp. 024108-16, 2011.

[11] X. Tang and B. Zheng, "A PDMS viscometer for assaying endoglucanase activity," *Analyst*, vol. 136, pp. 1222-1226, 2011.

[12] A. E. Mark and K. G. Bruce, "A PDMS-based gas permeation pump for on-chip fluid handling in microfluidic devices," *Journal of Micromechanics and Microengineering*, vol. 16, p. 2396, 2006.

[13] Y. N. Xia and G. M. Whitesides, "Soft lithography," *Annual Review of Materials Science*, vol. 28, pp. 153-184, 1998.

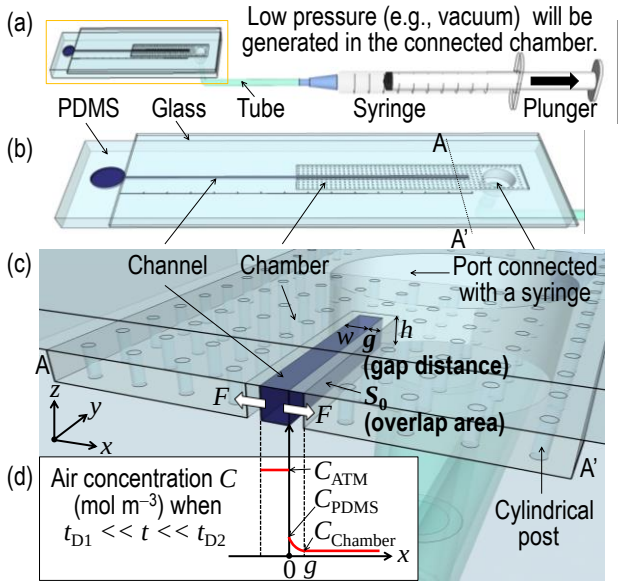

Figure 1: Schematic illustration of the proposed syringe-assisted point-of-care pumping: (a) the device connected with a syringe, (b) the glass-PDMS device, (c) three-dimensional view of the device, and (d) air concentration profile along the A-A' axis.

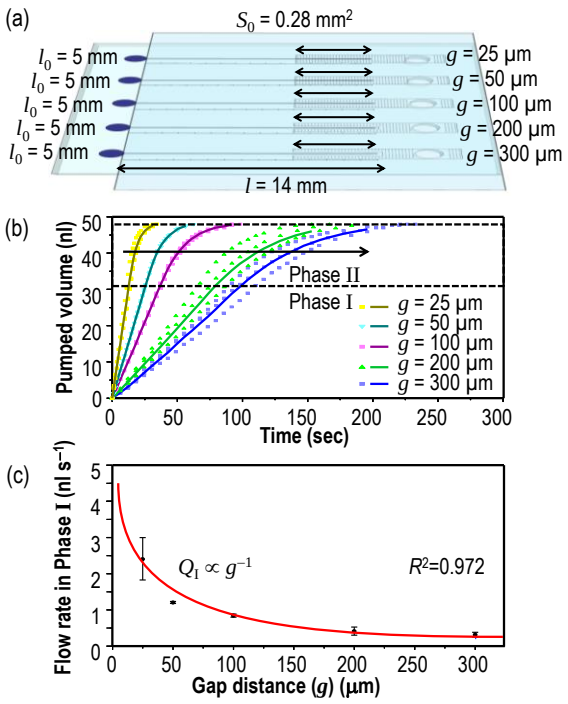

Figure 2: Effect of the gap distance between the channel and chamber on syringe-assisted pumping. (a) Schematic showing devices with varying gap distances (e.g., 25, 50, 100, 200 and 300 µm), while the overlap area is kept the same (S_0 = 0.28 mm^2). (b) Pumped volume profiles versus time with different gap distances. (c) Flow rate (Q_I) versus the gap distance (g) in Phase I.

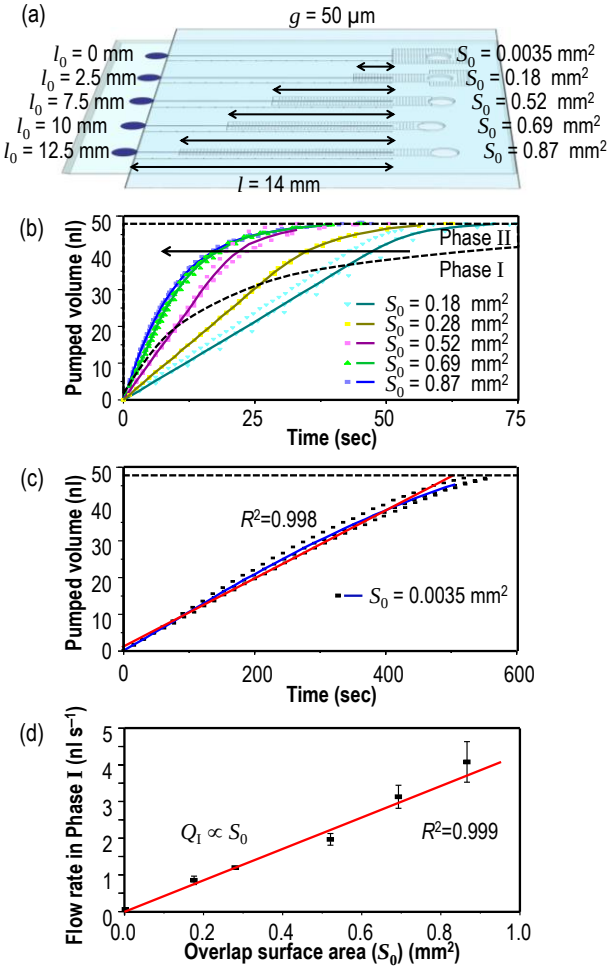

Figure 3: Effect of the overlap area between the channel and chamber on syringe-assisted pumping. (a) Schematic showing devices with varying overlap areas (e.g., 0.00345, 0.176, 0.521, 0.693 and 0.866 mm^2), while the gap distance is kept unchanged (g = 50 µm). (b and c) Pumped volume profiles versus time with different overlap areas. (d) Flow rate (Q_I) versus the overlap surface areas (S_0) in Phase I.